Copy
RM E52H08

NACA

RESEARCH MEMORANDUM

PERFORMANCE CHARACTERISTICS OF CANARD-TYPE MISSILE WITH VERTICALLY MOUNTED NACELLE ENGINES AT MACH NUMBERS 1.5 TO 2.0

By Leonard J. Obery and Howard S. Krasnow

Lewis Flight Propulsion Laboratory
Cleveland, Ohio

NATIONAL ADVISORY COMMITTEE
FOR AERONAUTICS

WASHINGTON
September 29, 1952

NATIONAL ADVISORY COMMITTEE FOR AERONAUTICS

RESEARCH MEMORANDUM

PERFORMANCE CHARACTERISTICS OF CANARD-TYPE MISSILE WITH VERTICALLY MOUNTED NACELLE ENGINES AT MACH NUMBERS 1.5 TO 2.0

By Leonard J. Obery and Howard S. Krasnow

SUMMARY

The over-all performance characteristics of a complete missile configuration were investigated in the Lewis 8- by 6-foot supersonic wind tunnel at Mach numbers 2.0, 1.8, and 1.5; angles of attack from 0° to 10°; canard-control-surface deflections from 0° to $9\frac{1}{2}^\circ$; and at a Reynolds number of approximately 6.9×10^6 based on wing mean aerodynamic chord. The missile had a canard-type control surface with nacelle-type engines mounted above and below the fuselage. The diffuser inlets were just ahead of the wing shock at the design Mach number of 2.0.

The investigation indicated that, at the design Mach number of 2.0, the addition of engines to the no-engine configuration increased the configuration drag and moved the aerodynamic center rearward but produced little additional lift. Control-surface deflection produced considerable pitching moment, but a large portion of the control-surface lift was lost because of the resultant downwash on the body and wing.

At zero angle of attack, the configuration drag was reasonably well predicted by existing theory with a body-engine interference drag experimentally determined from another model. At angle of attack, although the configuration lift and drag were also reasonably well predicted, the close agreement between theory and experiment resulted from compensating errors in the prediction of the control surface and engine lifts. Control-surface deflection adversely affected the lower-engine diffuser performance but had no effect on the upper engine except at the lowest Mach number.

INTRODUCTION

The performance of the component parts of an aircraft or missile may be calculated theoretically for moderate angles of attack and Mach numbers, or obtained experimentally. However, the prediction of the over-all performance of the missile from the component data will depend upon the interaction and interrelation of one component on another. This interaction may include the effects of the flow around the body on the diffuser characteristics as investigated in reference 1 or the effects of the relative positions of the components on drag as reported in references 2 and 3. Because of the complicated nature of the air flow, the interference effects shown in these references are very difficult to calculate analytically.

Therefore, an investigation was conducted to determine the complete-configuration performance of a representative-type missile. This missile had a canard-type control surface with nacelle engines mounted above and below the fuselage at a rearward body station. The purpose of the investigation was to determine (1) the over-all force and moment characteristics of a specific configuration and to indicate the effect of each component on the configuration performance and (2) the diffuser performance of the engines as affected by the missile components.

The investigation was conducted in the Lewis 8- by 6-foot supersonic wind tunnel at Mach numbers 2.0, 1.8, and 1.5 through a range of angles of attack, control-surface deflections, and engine mass-flow ratios. The Reynolds number of the investigation was approximately 6.9×10^6 based on wing mean aerodynamic chord.

SYMBOLS

The following symbols are used in this report:

b	wing span, 52 in.
C_D	drag coefficient, D/q_0S
C_L	lift coefficient, L/q_0S
C_M	pitching-moment coefficient about station 58, moment/$q_0S\bar{c}$
c	chord of wing

$\bar{c}$ mean geometric chord of wing, defined by $\dfrac{\int_0^{b/2} c^2 dy}{\int_0^{b/2} c\, dy}$, 17.97 in.

D drag, lb

L lift, lb

M Mach number

m_2/m_0 mass-flow ratio, unity when free-stream tube as defined by cowl lip enters engine

P total pressure

p static pressure

q_0 free-stream dynamic pressure, $\gamma p_0 M_0^2/2$

S total wing plan-form area, 900 sq in.

y distance along wing in spanwise direction measured from fuselage center line

α angle of attack, deg

γ ratio of specific heats, 1.4

δ canard-control-surface deflection from body center line, positive deflection same sense as positive angle of attack

Subscripts:

0 free stream

2 engine diffuser exit

APPARATUS AND PROCEDURE

The model investigated in the tunnel consisted of a body of revolution with a canard-type control surface, a wing, and a nacelle engine

mounted at a rearward station in the vertical plane (fig. 1). The symmetrical body had a length-diameter ratio of 12 and a maximum diameter of 9 inches.

The wing was of trapezoidal plan form with a total area of 900 square inches and an exposed area of approximately 712 square inches, and had an aspect ratio of 3, a taper ratio of 0.5, and an unswept 50-percent chord line. The airfoil section was a double circular arc of 5-percent thickness ratio.

The control surface was similar to the wing, with the exception that the thickness was increased to 8 percent near the root for structural reasons. It had a total plan area of 135 square inches, or 15 percent of the total wing area. The all-movable surface was hinged about its 50-percent chord line and was remotely operated. The nose portion of the body adjacent to the forward half of the control surface was fixed to and deflected with the surface.

The engine was located $1\frac{1}{2}$ engine diameters below the body center line. It was designed to achieve low drag characteristics and was identical to the straight-taper-cowl engine discussed in detail in reference 1. The engine mass flow was controlled by means of a movable plug mounted independently of the model and the tunnel balance system.

Limitations imposed by the support system made it impossible to test directly the configuration being investigated. From the models actually tested (fig. 2(a)), the characteristics of the complete configuration (fig. 2(b)) were computed. The engine - strut combination of the test model, when operated at negative angles of attack and negative control deflections, is equivalent to the upper engine - strut combination of the complete configuration at positive angles of attack and control deflections. Furthermore, the external characteristics of the engine - strut could be evaluated by subtracting the characteristics of the test model without engine from those of the test model with engine at any given condition. These values were added to the test model at the appropriate angle of attack and control deflection to obtain the characteristics of the complete configuration.

Instrumentation for the engine consisted of static-pressure rakes located at the diffuser exit and in the combustion chamber. Two independent force-measuring techniques were utilized in the investigation. The first was the tunnel-support-scale system to which the model and support strut were directly connected; this system was used to determine the lift and drag data presented herein. The strut drag tares were determined experimentally by measuring the forces developed by a combination of the strut and a bullet-shaped body of known drag. For the configuration without engines, a slight negative lift was measured at

$\alpha = 0^\circ$ and $\delta = 0^\circ$ and was believed to result from a pressure gradient developed by the support strut acting on the wing. Accordingly, a constant angle of attack correction was made to the lift and drag data for all configurations. A possibility of drag interference also existed for all configurations because of the support strut; however, this interference was believed to be negligible for all conditions. Reflected waves from the tunnel walls were believed to touch only a small part of the wing at $M_0 = 2.0$; and at $M_0 = 1.5$, the effect was believed to be limited to a small amount of reflected upwash on the wing, about 0.2° at $\alpha = 0^\circ$ and $\delta = 10^\circ$. Difficulties encountered in evaluating the strut tare for moment necessitated using the second measuring system. The model was connected to the support strut through two links located 15 inches apart upon which were mounted electrical strain gages. From a calibration of these gages, the moment acting on the model was determined directly. The zero lift drag as measured by the strain gages also agreed closely with the drag as determined from the tunnel scales, which indicates that the strut tares were accurately known. However, interaction effects of lift on the drag strain gage caused the strain-gage data to be unusable at angle of attack.

In the reduction of the data, the forces and moments developed by the engine internal flow were removed from the measured values. The lift and drag contributed by the engine internal flow were computed from the engine thrust (including the entering free-stream momentum). In the determination of the moment developed by the engine internal flow, the assumptions were made that the engine thrust acted on the engine center line and that the momentum change due to the turning of the entering free-stream tube occurred at the cowl lip. Thus the forces and moment presented are independent of the engine performance and were developed entirely by the air flow external to that entering the engines. The mass flow through the engine was determined from the known open area at the exit and the combustion-chamber static pressure with the assumption that the exit area was choked. The diffuser total-pressure recovery was determined from the known mass flow and the diffuser-exit static pressure.

DISCUSSION

Force and Moment Evaluation

Because of the manner of testing, it was necessary to determine the characteristics of the model without engines. The forces and moments developed by this configuration (which might be representative of a rocket-powered aircraft or a glide missile) are presented in figure 3 as a function of angle of attack for three Mach numbers. The drag of the configuration increased rapidly with angle of attack and at a given angle of attack increased considerably with control deflection. For control

deflections greater than zero the drag curves are asymmetrical about $\alpha = 0$ and indicate that the minimum drag for these conditions would be at some negative angle of attack. The lift curves were linear with angle of attack, and the slopes increased with decreasing Mach number. At a given angle of attack, control deflection increased the configuration lift, although not as much as might be expected from the control-surface lift. However, the control was very effective in producing pitching moment as shown by the large increase in C_M with control deflection at a given angle of attack. Also, as the Mach number was reduced the control effectiveness increased because of the increased control lift at the lower Mach numbers. The longitudinal stability of the configuration increased slightly with decreasing Mach number as shown by the increasingly negative moment slopes.

The force and moment characteristics of the model with engines (hereinafter called the complete configuration) are presented in figure 4 for critical or supercritical engine operation. For both configurations, it was assumed that the center of gravity was located at station 58, and accordingly the moment center was located at this station. This was also as far rearward as the moment center could be moved while model stability was maintained at all conditions. As with the previous configuration, control deflection increased the drag and pitching moment considerably but had a lesser effect on lift; in general, the trends of the curves are similar for both configurations. The addition of the engines increased the drag, but at the higher Mach number very little extra lift was obtained from the engines, as can be seen from a comparison of figures 3 and 4. The engines, however, moved the aerodynamic center rearward, as evidenced by a comparison of the slopes of the pitching-moment curves for the two configurations.

The lift-drag ratios for the complete configuration are shown in figure 5 as a function of angle of attack. Increasing the control deflection reduced the maximum lift-drag ratio, since the control surface increased the model drag by a greater percentage than it increased the lift. Also, decreasing the Mach number increased the maximum lift-drag ratios.

The component drags of the complete configuration at zero angle of attack and zero control deflection were calculated theoretically, and the combinations of these components were determined experimentally (fig. 6). The body was of the Haack type (minimum drag for a given length and volume); the theoretical wave drag is given in reference 4 for the case I body. The friction drag of the body was determined from reference 5. As shown in figure 6, although the experimental body drag was somewhat lower than predicted, the agreement was quite good at all Mach numbers. The pressure drag of the control surface, the wing, and the engine struts was determined from two-dimensional potential flow theory, and the tip effects of the control surface and the wing were

estimated from reference 6. The friction drag of these components was determined from reference 5. As shown from the incremental drags, the control-surface and the wing drag coefficients were predicted quite accurately; and except for the lowest Mach number the summation of predicted body, control-surface, and wing drags agreed quite well with the experimentally determined values, although interference effects were neglected in the calculations. The theoretical pressure drag for the engines was calculated from reference 7; the additive drag at Mach number below 2.0, from reference 8; and the engine friction drag, from reference 5. The summation of the theoretical drag coefficients was considerably greater than the experimental value, as shown by comparison of the dash-3-dot line and the triangular data points. This difference is due in part to the favorable engine-body interference drag as shown in references 2 and 3. The interference-drag factor was determined from the experimental results of reference 2, and the addition of this term to the theoretical summation shows that the predicted and experimental drag coefficients are in reasonably good agreement throughout the Mach-number range. The experimental rather than the theoretical interference-drag factor was used in this report, because, as is shown in reference 2, the theoretical analysis predicts the correct trends but does not predict the absolute value of the interference factor with sufficient accuracy.

The theoretical values of lift and drag at angle of attack were also determined for zero control deflection and are presented with the experimental values in figure 7. The lift of the control surface was determined from potential theory with approximate tip corrections, and the engine lift was determined by the method of reference 9. The lift of the body and wing combination was determined from references 10 and 11.

From the comparison of experiment and theory, it is evident that at all Mach numbers the lift due to control surface deflection was considerably overestimated by theory. Still, the comparison is not entirely justified, since (as will also be discussed later) the downwash effect of the control surface on the body and wing is included in the experimentally determined control-surface lift. However, since that lift resulted from control deflection, it was used as such in the breakdown of component lift.

At a Mach number of 2.0, the engine lift was overestimated by the method of reference 9, and it is evident that the lift contributed by the engines is quite small. However, at the lower Mach numbers the engine lift was underestimated. It should be noted that the engine lift as determined experimentally included all the lift interference of the engines and body and also the contribution of the additive drag incurred at angle of attack, and hence may not be expected to agree exactly with

theory. In general, it was determined that at positive angles of attack the upper engine had much lower lift values than the lower engine, and at the higher Mach numbers the upper engine even produced negative lift.

The predicted values (references 10 and 11) of body and wing lift agreed quite closely with those obtained experimentally. The theory does not consider any loss in body lift due to the converging afterbody shape; however, as a compensating condition, neither does it account for crossflow separation, and the two effects might tend to cancel. Because the main lift comes from the wing, these effects may be rather insignificant.

At all Mach numbers, the summation of the theoretically determined lift agreed quite closely with the experimental value. However, at the lower Mach numbers it is evident that the close agreement resulted from compensating errors in the predicted values of engine and control-surface lifts. Since the body and wing lift was such a major portion of the total lift, it is more important that this value was predicted so closely.

The theoretical drag at angle of attack was determined from the addition of the induced drag to the zero lift-drag from figure 6. As seen in the theoretical and experimental drag comparison (fig. 7), the experimental drag was underestimated for all Mach numbers at the higher angles of attack. Since the lift was predicted quite closely, it might be expected that the drag would have been predicted even more closely. However, the axial force, which was assumed constant for the theoretical calculation and equal to the drag at zero angle of attack, increased considerably at angle of attack. It is believed that the favorable drag interference created by the relative location of engines and body was entirely lost as the model went to angle of attack.

As was mentioned previously, the control surface added only a small amount of lift but a substantial pitching moment to the configuration. It was expected that the control surface was developing considerable lift but that some of that lift was lost because of the action of the control-surface downwash on the body and wing. This presumption is confirmed by the data of figure 8, which shows that the actual amount of lift developed by the configuration due to control deflection was markedly less than the theoretical lift of the control surface. As a comparison the control-surface lift (i.e., the lift that the control surface developed without regard to the resultant downwash) was also calculated by assuming that, at zero angle of attack, all the pitching moment of the missile was produced by the control surface. It was further assumed that the center of lift was at the midchord of the control, and thus the control-surface lift was calculated from the measured configuration moment and the assumed distance. Comparison of the control lift so calculated with the theoretical lift shows good agreement

and indicates that the pitching moment could be calculated accurately from the theoretical control-surface lift. It is evident that, while the forward control surface is a good moment-producing device, a large part of its lift may be lost because of downwash on the body and wing.

The minimum engine drag coefficient (critical or supercritical engine operation) developed by the upper and lower engines and their supporting struts is presented in figure 9. Also included in the engine drag is the body-engine interference drag. The lower-engine drag coefficient increased considerably with angle of attack but was independent of control deflection. At the lower Mach numbers, increasing the angle of attack caused a decrease in the upper-engine drag coefficient; and except at $M_0 = 1.5$, increasing the control deflection increased the upper-engine drag coefficient.

The effect of varying the engine mass flow on engine drag coefficient is shown in figure 10. Because of the additive drag associated with subcritical engine operation, both the upper- and lower-engine drag coefficients increased with decreased mass-flow ratio; but the percentage increase in configuration drag was notably less than the increase in engine drag. For example, at $M_0 = 2.0$ and $\alpha = 3^\circ$ the mass flow for both engines could be reduced 13 percent (about the limit of the diffuser stable subcritical range), corresponding to approximately 66-percent increase in engine drag but only a 12-percent increase in configuration drag. These data apply directly to the engine drag at zero control deflection. For the two conditions at which the engine drag was not independent of control deflection, that is, upper engine at M_0 of 2.0 and 1.8 (fig. 9), the increment of drag from critical mass-flow ratio to any desired mass-flow ratio may be added to these engine-drag curves to obtain the engine drag at the desired mass-flow ratio and control deflection. Data not presented in this report indicate that changes in mass-flow ratio had little or no effect on the lift and pitching-moment coefficients of the configuration.

Engine-Internal-Flow Evaluation

The diffuser characteristics of the upper and lower engines are shown in figure 11. Included for convenience in the figure is the diffuser-exit Mach number M_2. At a Mach number of 2.0 (fig. 11(a)) the lower engine was more seriously affected by angle of attack in both pressure recovery and mass-flow ratio than was the upper engine. Control deflection also adversely affected the lower engine at the lower angles of attack, but had no effect on the upper engine. It is not evident why control deflection had no effect on the upper-engine characteristics, since it might be expected that the trailing-tip vortices from the control would influence the upper engine (see reference 1).

At a Mach number of 1.8 (fig. 11(b)), in contrast to results at the higher Mach number, angle of attack influenced the upper engine more severely than the lower. It is believed that this reversal of trend resulted from the shock from the wing leading edge, which remained ahead of the inlet at a Mach number of 1.8, but which intersected the diffuser cowl at Mach number 2.0. At Mach number 1.8 the compression shock from the under surface of the wing turned the flow toward the lower-engine axis and also reduced the Mach number ahead of the inlet. The upper-engine inlet, however, was not located in this type of alleviating environment. At Mach number 2.0, because the inlets were ahead of the wing shock, these effects were not noted. Again as at a Mach number of 2.0, control deflection adversely affected the lower-engine performance but had no apparent effect on the upper engine.

At a Mach number of 1.5 (fig. 11(c)) angle of attack had relatively little effect on either the upper or lower engine; but as with the higher Mach numbers, control deflection again had a greater adverse effect on the lower engine than on the upper engine. It is interesting that at 7°, the highest angle of attack for the upper engine, control deflection did affect the upper-engine performance. Very possibly, if the upper-engine angle of attack could have been increased beyond 7° at the higher Mach numbers, control deflection might have influenced the upper-engine performance.

SUMMARY OF RESULTS

An investigation was conducted in the 8- by 6-foot supersonic wind tunnel to determine the performance characteristics of a complete missile configuration at Mach numbers 2.0, 1.8, and 1.5 and a Reynolds number of approximately 6.9×10^6 based on wing mean aerodynamic chord. The missile had a canard-type control surface with nacelle engines mounted above and below the fuselage. The inlets were mounted close to the body and at a rearward station just ahead of the wing shock at the design Mach number of 2.0.

The following results were obtained:

1. Addition of engines measurably increased the configuration drag and also moved the missile aerodynamic center rearward but had less effect on lift at the design Mach number.

2. Maximum lift-drag ratio increased with decreasing M_0 but decreased with increasing control deflection.

3. The zero lift drag of the body, control surface, and wings was reasonably well predicted by existing theory. Addition of the

theoretical engine and strut drag and an experimental engine-body interference drag to the other component drags gave reasonable agreement between predicted and experimental configuration drag.

4. The lift of the body-wing combination was reasonably well predicted by existing theory. The component lifts of engines and control surface were not predicted, but the compensating errors in these values yielded good over-all agreement for the configuration.

2631

5. At the high angles of attack, the drag of the configuration was underestimated, possibly because of an increase in the experimental axial forces.

6. The pitching moment produced by the control surface could be calculated accurately from the theoretical control-surface lift even though a large part of the lift was lost because of downwash on the body and wing.

7. Control deflection had little effect on the lower-engine drag for supercritical flow, but at the higher Mach numbers it did increase the upper-engine drag. Increased angle of attack caused a decreased upper-engine drag at the lower M_0.

8. Control-surface deflection adversely affected the pressure recovery and mass-flow ratio of the lower engine but had no effect on the upper engine except at the lowest Mach number.

Lewis Flight Propulsion Laboratory
National Advisory Committee for Aeronautics
Cleveland, Ohio

REFERENCES

1. Obery, L. J., and Krasnow, H. S.: Influence of a Canard-Type Control Surface on the Internal and External Performance Characteristics of Nacelle-Mounted Supersonic Diffusers (Conical Centerbody) at a Rearward Body Station for a Mach Number of 2.0. NACA RM E52F16, 1952.

2. Kremzier, Emil J., and Dryer, Murray: Aerodynamic Interference Effects on Normal and Axial Force Coefficients of Several Engine-Strut-Body Configurations at Mach Numbers of 1.8 and 2.0. NACA RM E52B21, 1952.

3. Friedman, Morris D.: Arrangement of Bodies of Revolution in Supersonic Flow to Reduce Wave Drag. NACA RM A51I20, 1952.

4. Jones, Robert T.: Estimated Lift-Drag Ratios at Supersonic Speeds. NACA TN 1350, 1947.

5. Tucker, Maurice: Approximate Calculation of Turbulent Boundary-Layer in Compressible Flow. NACA TN 2337, 1951.

6. Nielsen, Jack N.: Effect of Aspect Ratio and Taper on the Pressure Drag at Supersonic Speeds of Unswept Wings at Zero Lift. NACA TN 1487, 1947.

7. Jack, John R.: Theoretical Wave Drag and Pressure Distribution for Axially Symmetric Open-Nose Bodies. NACA TN 2115, 1950.

8. Sibulkin, Merwin: Theoretical and Experimental Investigation of Additive Drag. NACA RM E51B13, 1951.

9. Allen, H. Julian: Estimation of the Forces and Moments Acting on Inclined Bodies of Revolution of High Fineness Ratio. NACA RM A9I26, 1949.

10. Nielsen, Jack N., and Kaattari, George E.: Method for Estimating Lift Interference of Wing-Body Combinations at Supersonic Speeds. NACA RM A51J04, 1951.

11. Lagerstrom, Paco A., Wall, D., and Graham, M. E.: Formulas in Three-Dimensional Wing Theory (1). Rept. No. SM-11901, Douglas Aircraft Co., Inc., July 8, 1946.

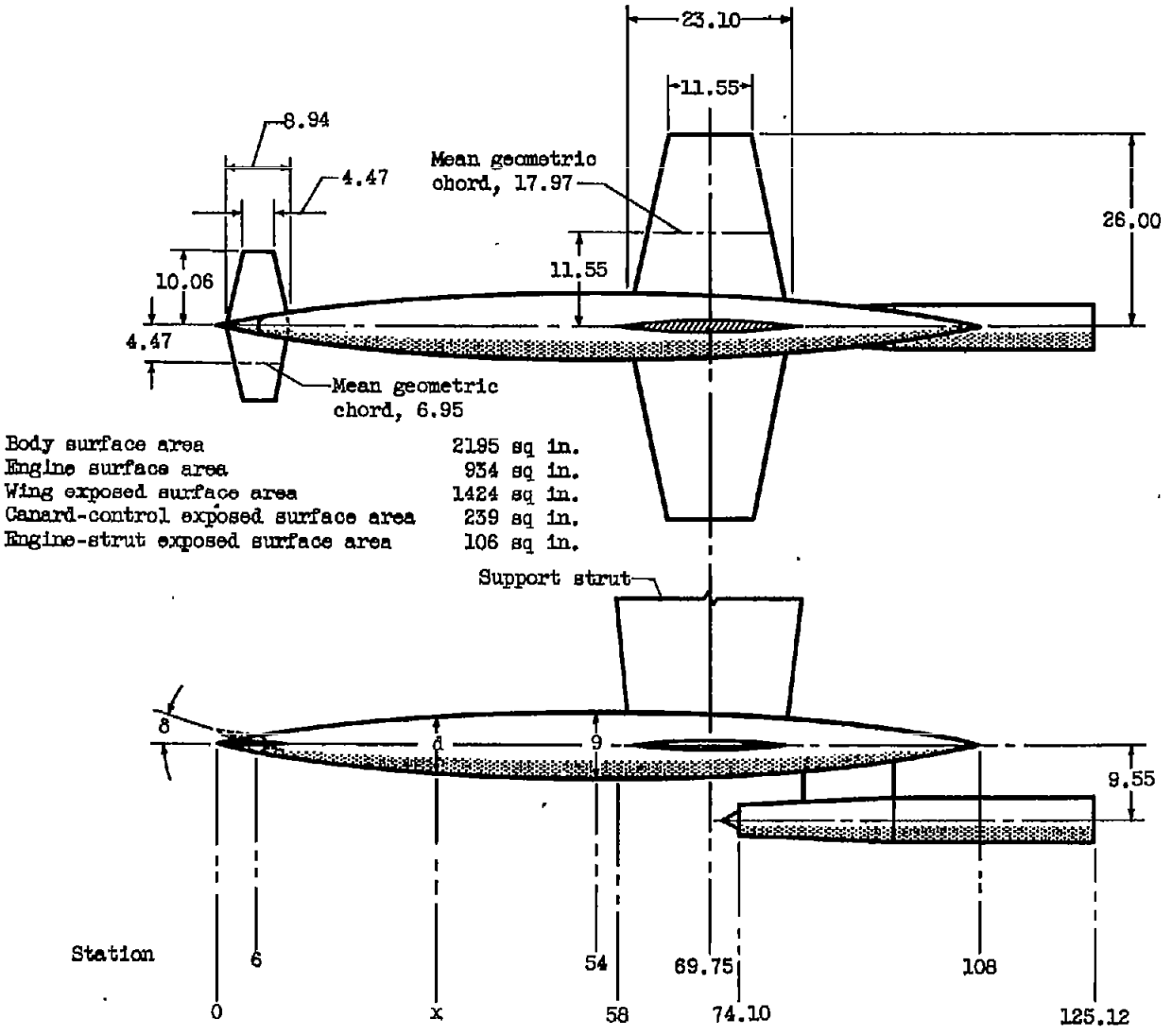

NACA CD-2750

Figure 1. - Sketch of model as tested in tunnel. Body defined by $d = 9\left[1 - (1-x/54)^2\right]^{3/4}$, inches. (All dimensions in inches.

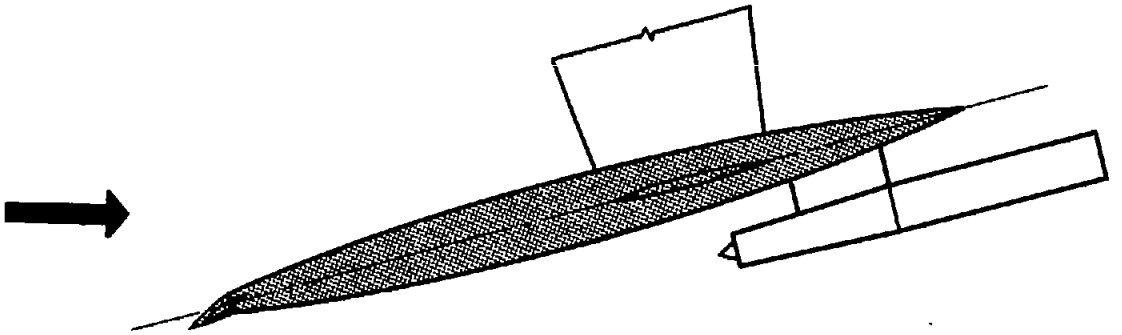

(a) Models as tested in tunnel. Shaded portion for body, wing, and control-surface test.

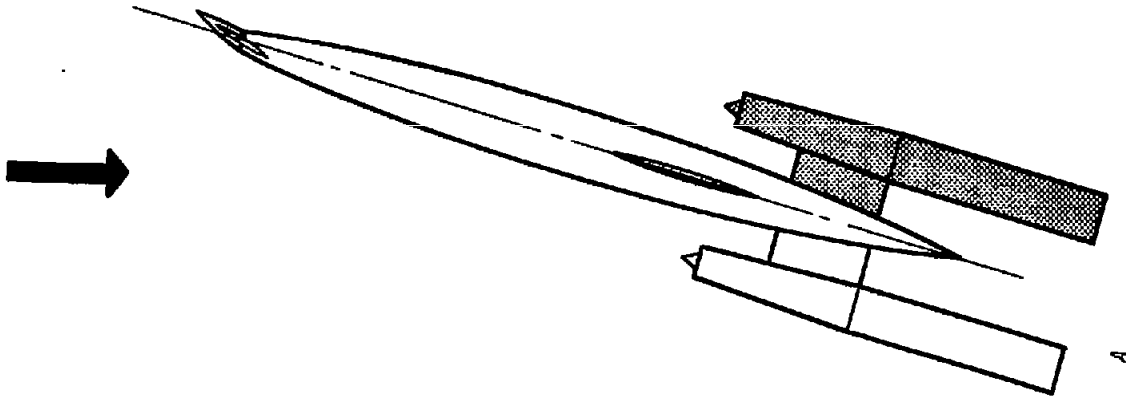

(b) Complete configuration. Performance of shaded engine determined by computation from tested models.

Figure 2. - Sketch of test models and complete configuration.

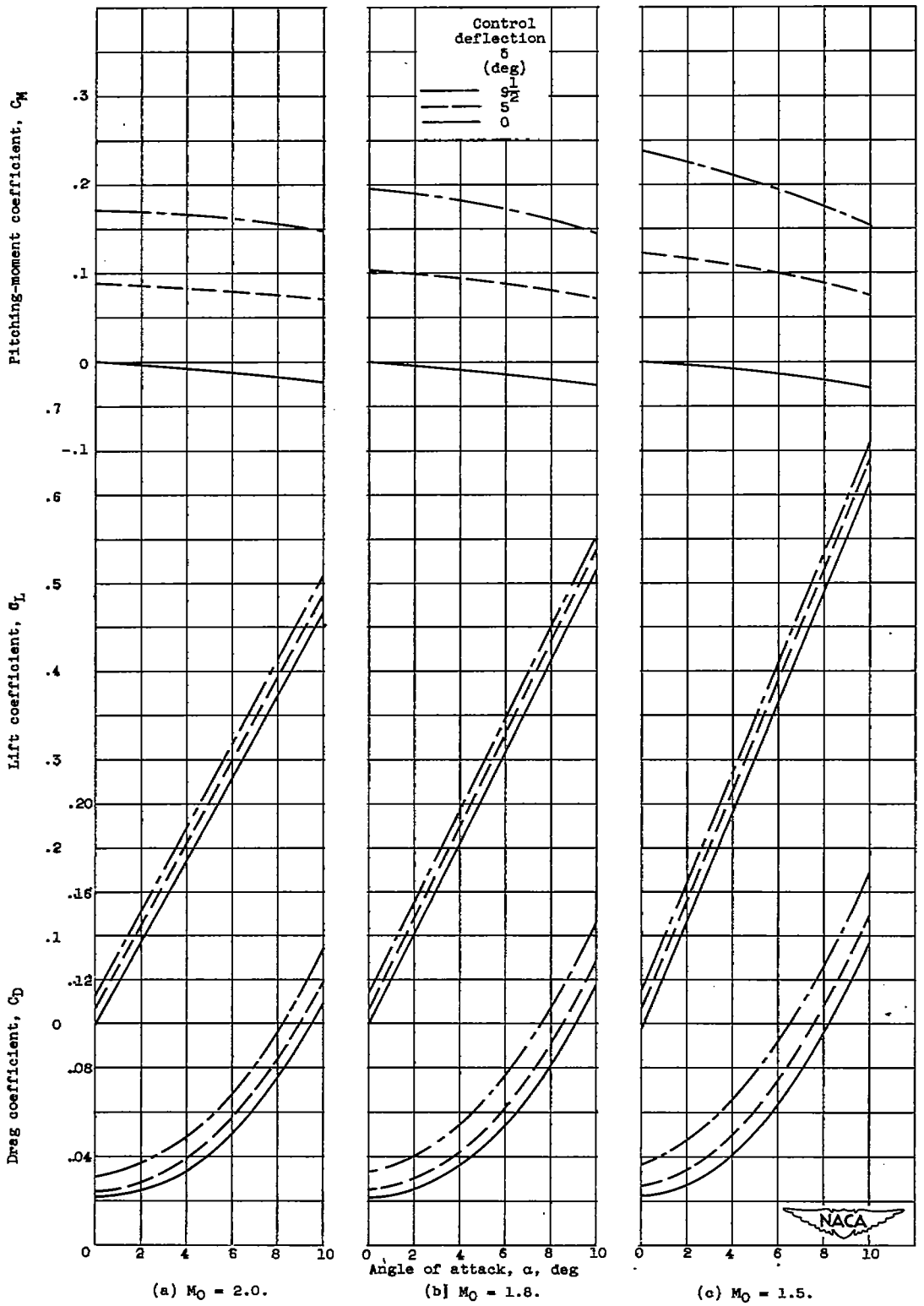

(a) M_O = 2.0. (b) M_O = 1.8. (c) M_O = 1.5.

Figure 3. - Variation of drag, lift, and pitching moment with angle of attack for body, wing, and control-surface configuration for several control deflections at three Mach numbers.

[redacted]

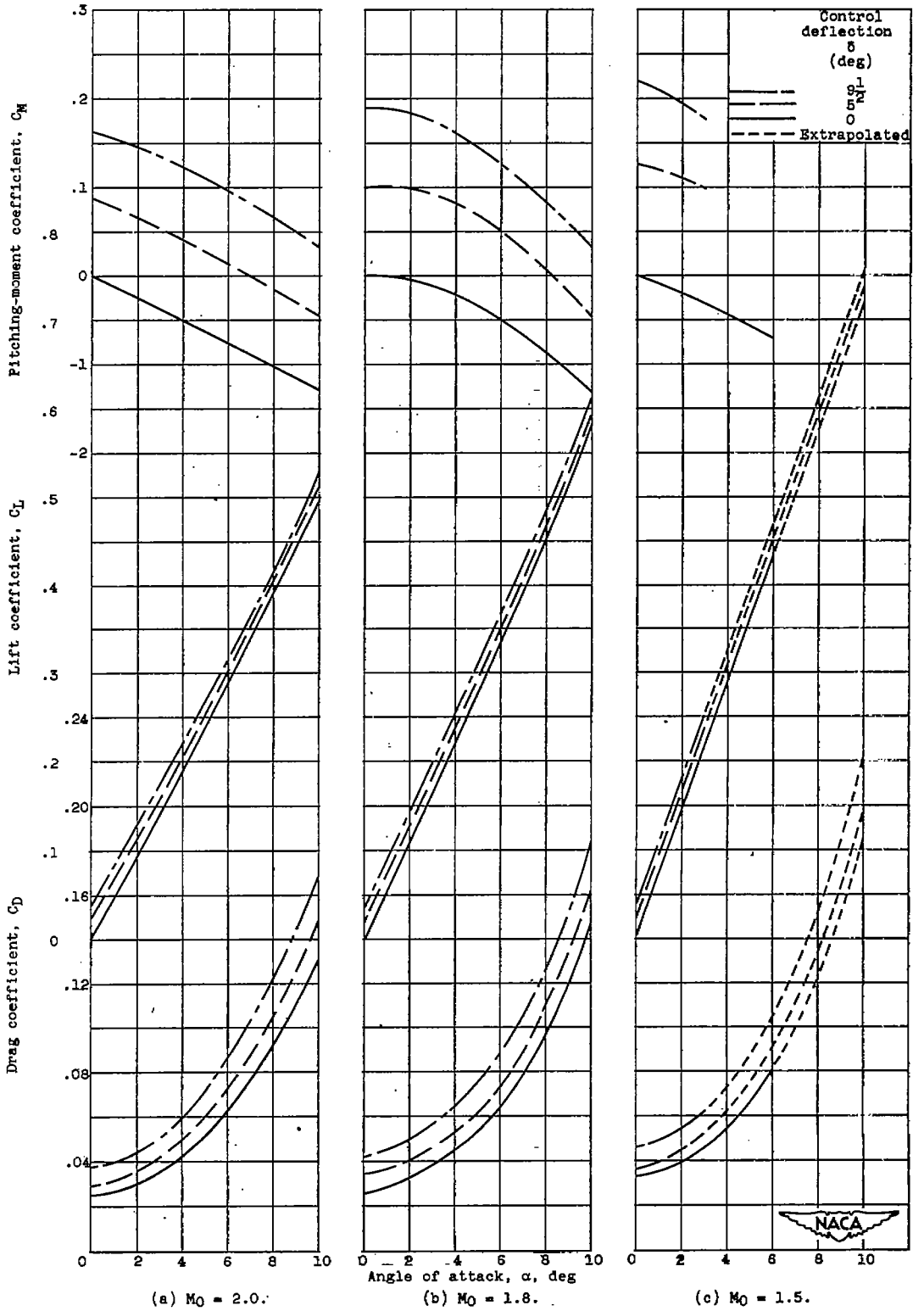

Figure 4. - Variation of drag, lift, and pitching-moment coefficients with angle of attack for complete configuration for several control deflections and three Mach numbers.

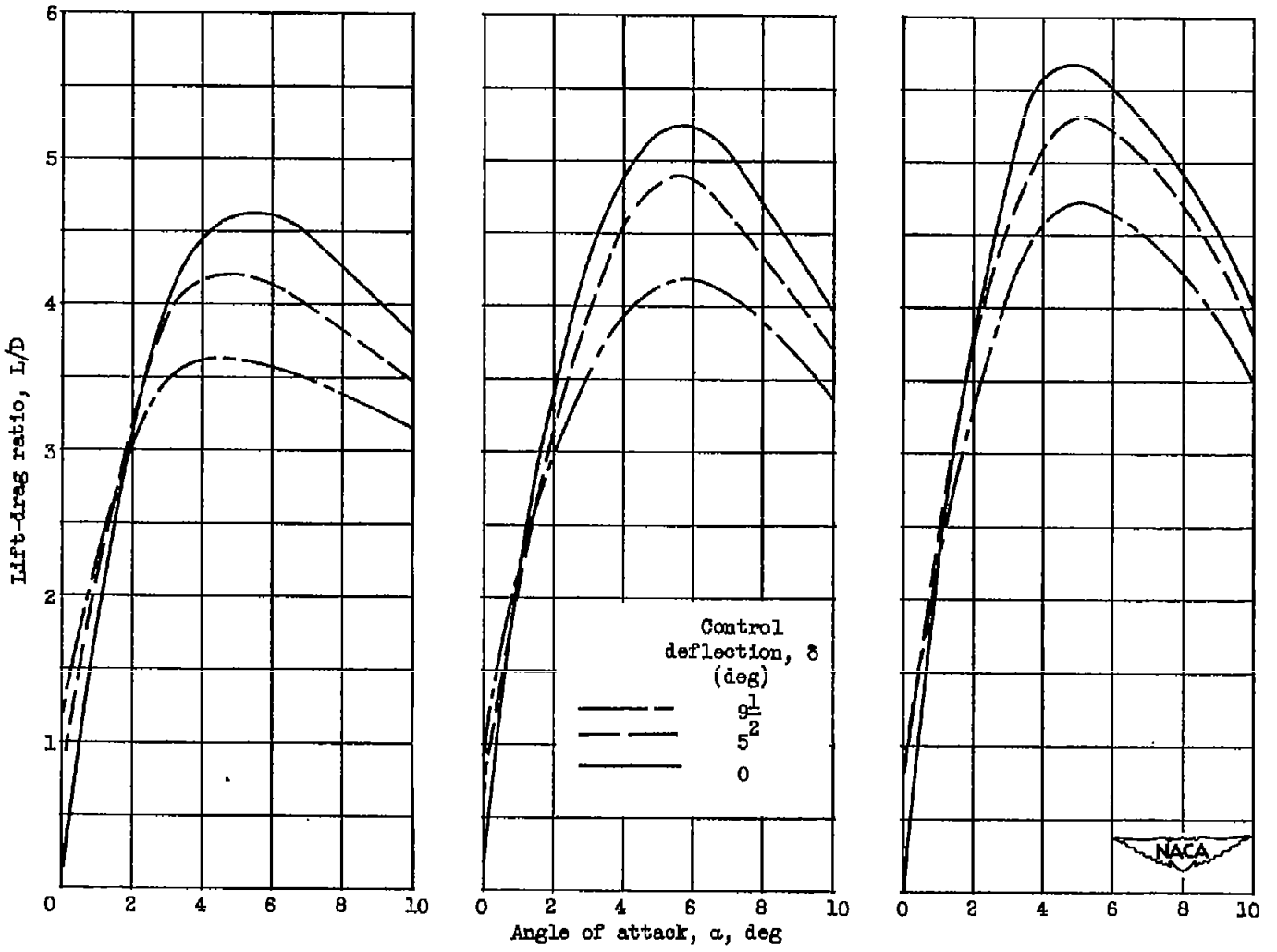

(a) $M_0 = 2.0$ (b) $M_0 = 1.8$. (c) $M_0 = 1.5$.

Figure 5. - Variation of lift-drag ratio with angle of attack for complete configuration for several control deflections at three Mach numbers.

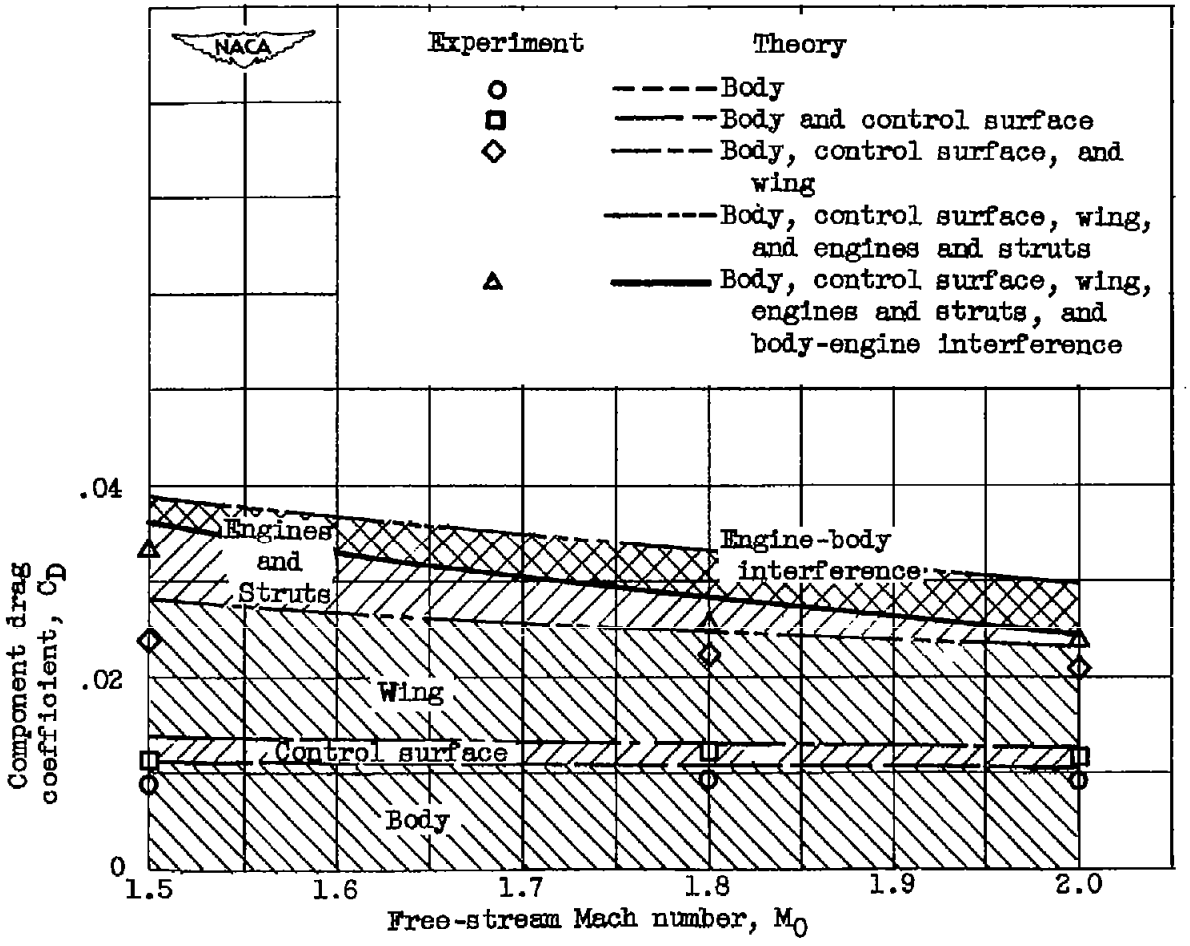

Figure 6. - Variation of experimental and theoretical component drag coefficients with free-stream Mach number for zero control-surface deflection and zero angle of attack.

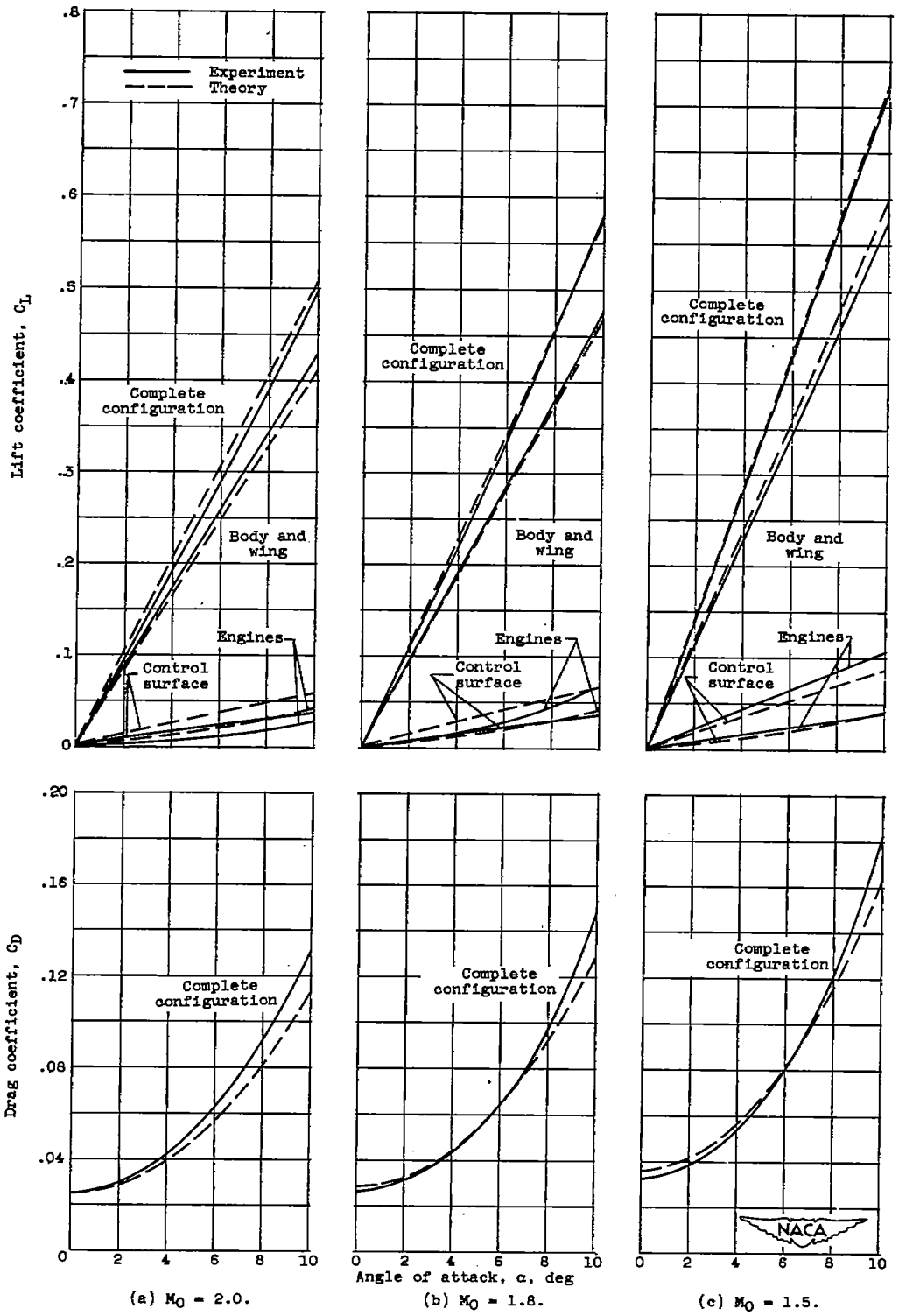

Figure 7. - Experimental and theoretical variation of lift and drag coefficients with angle of attack for three Mach numbers at zero control deflection.

[redacted]

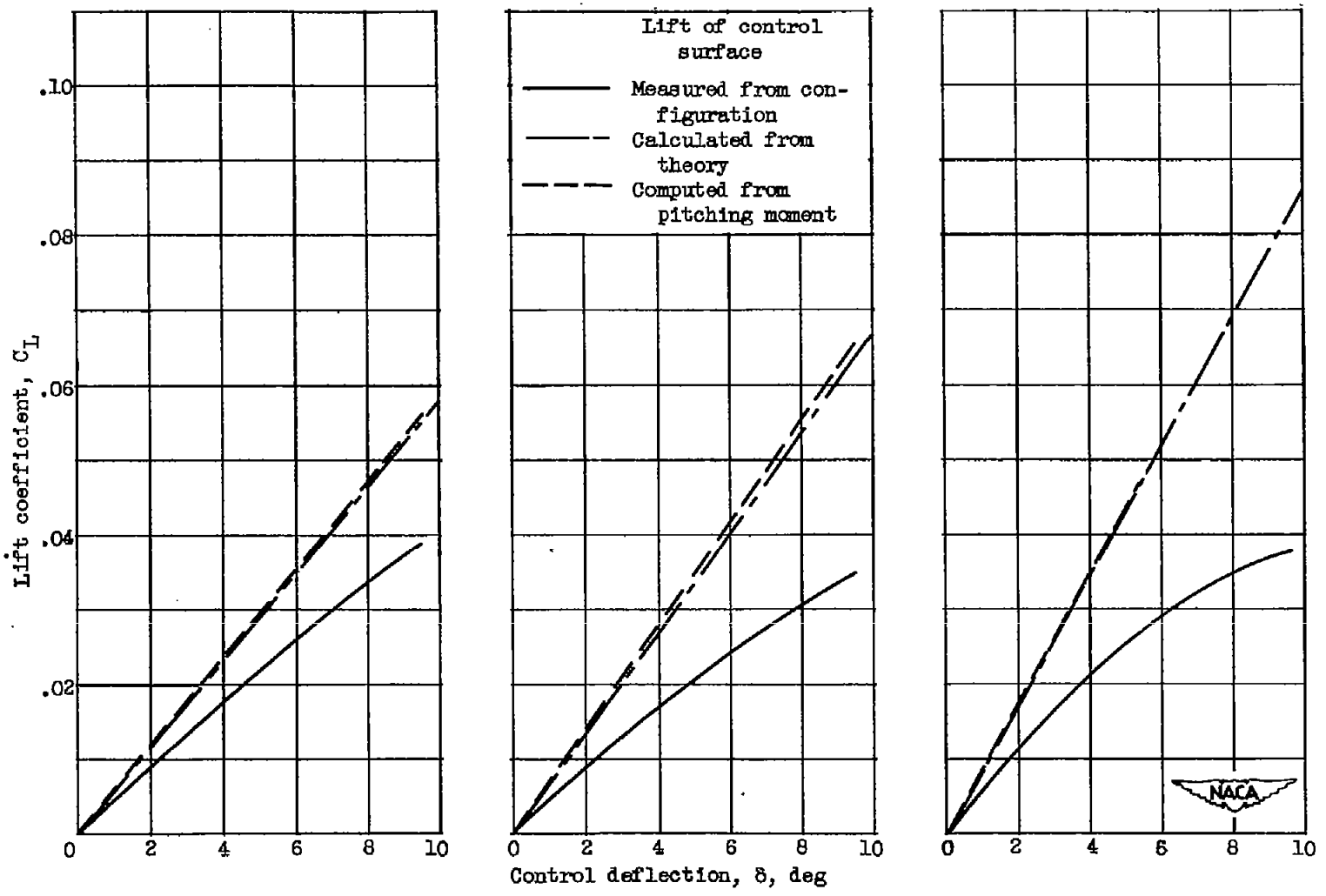

(a) M_0 = 2.0. (b) M_0 = 1.8. (c) M_0 = 1.5.

Figure 8. - Variation of control-surface lift with control deflection as measured from complete configuration, calculated from theory, and computed from pitching moment for several Mach numbers at zero angle of attack.

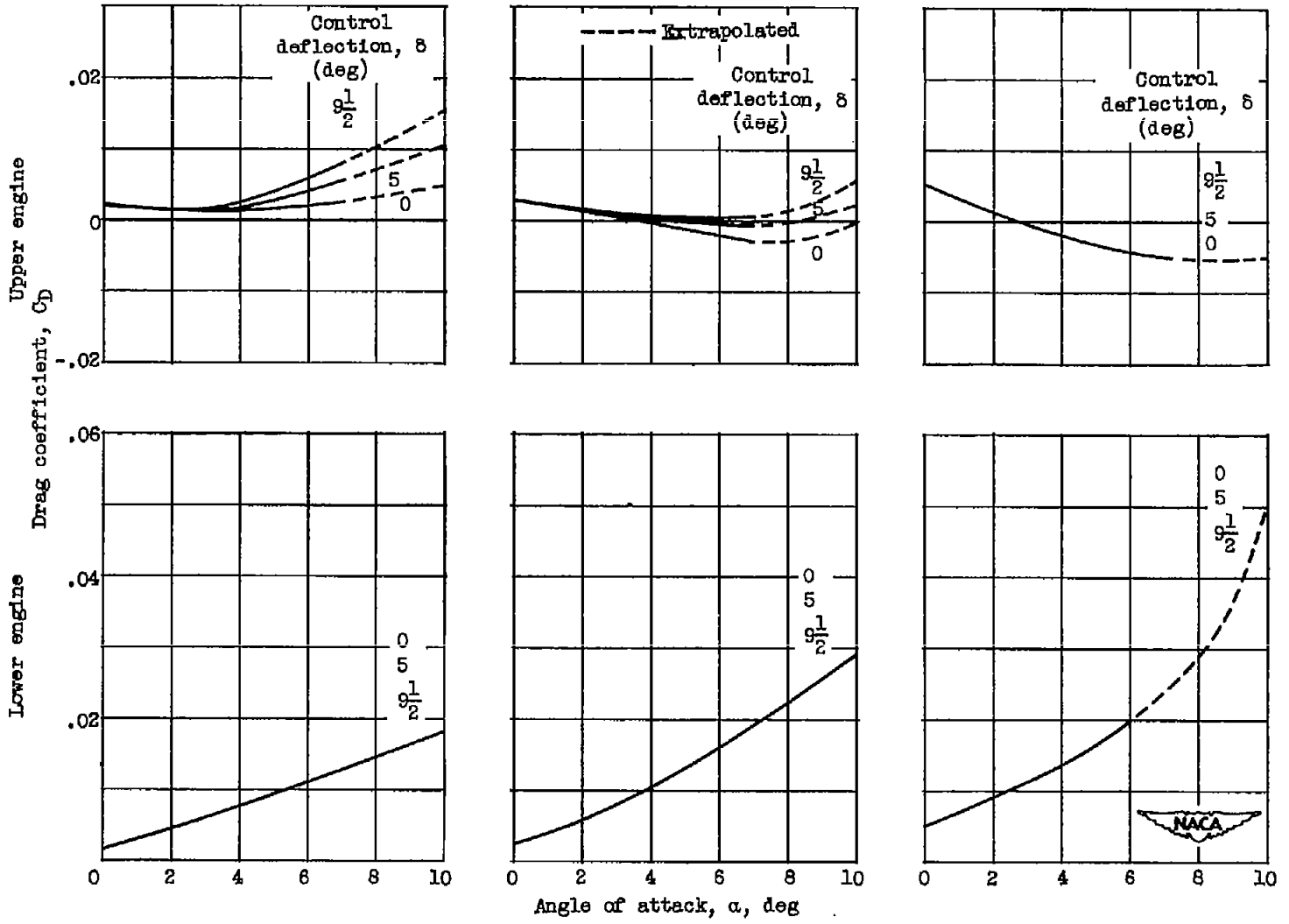

(a) $M_0 = 2.0$. (b) $M_0 = 1.8$. (c) $M_0 = 1.5$.

Figure 9. - Variation of engine - strut drag coefficient (critical mass-flow ratio) with angle of attack for several control deflections at three Mach numbers.

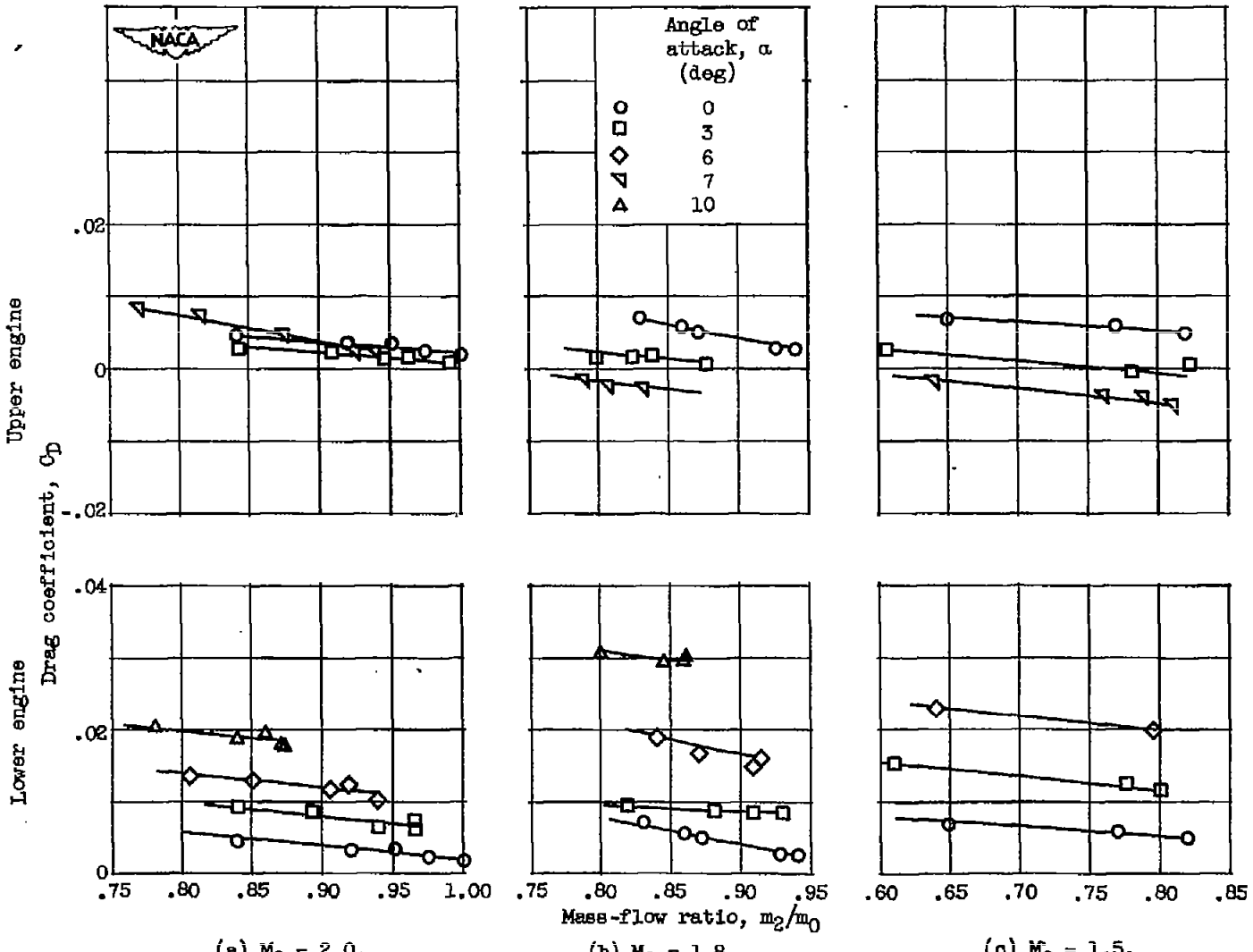

(a) M_0 = 2.0. (b) M_0 = 1.8. (c) M_0 = 1.5.

Figure 10. - Variation of engine - strut drag coefficient with mass-flow ratio for zero control deflection at several angles of attack for three Mach numbers.

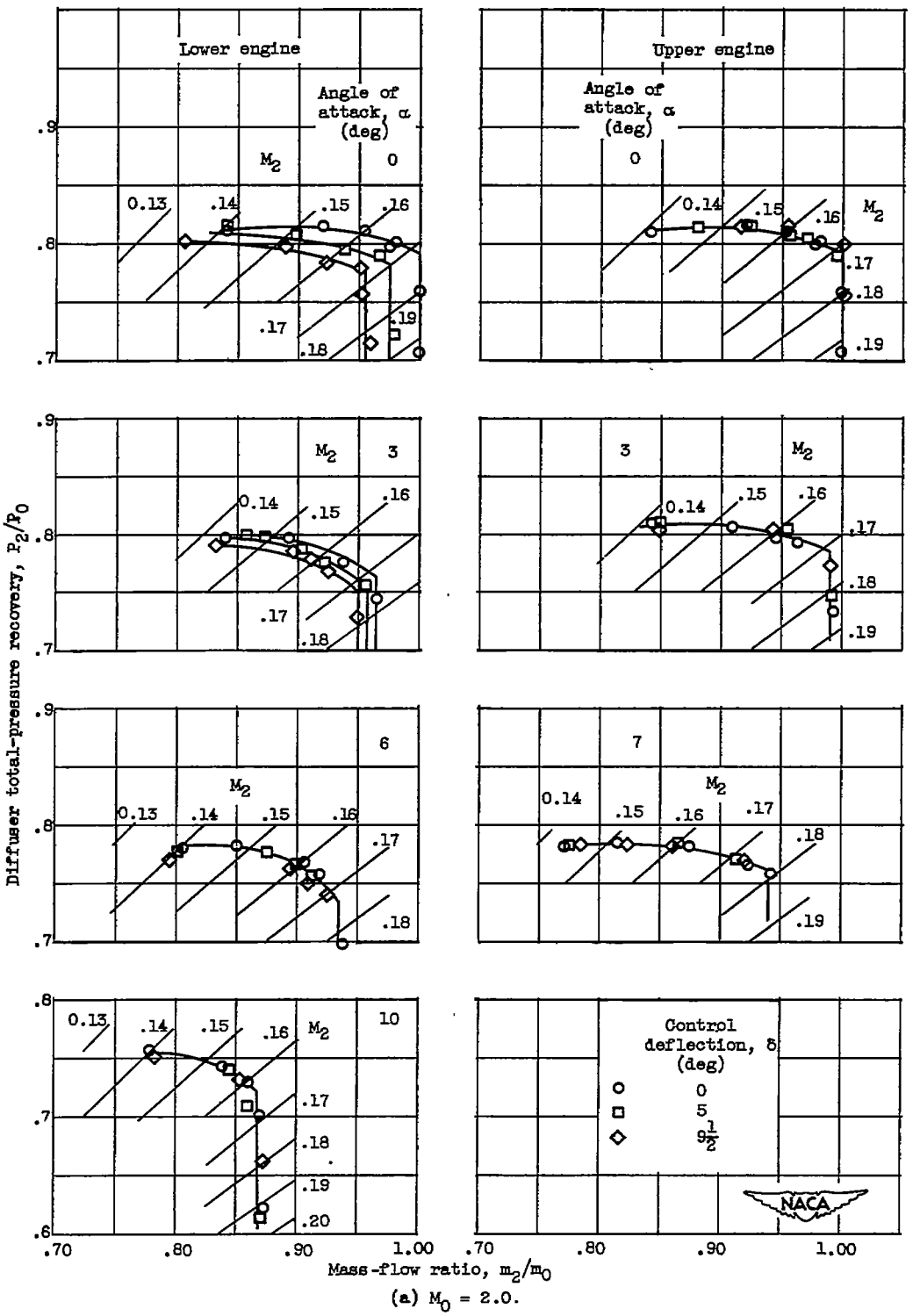

(a) $M_0 = 2.0$.

Figure 11. - Variation of total-pressure recovery with mass-flow ratio for upper and lower engines at several angles of attack for three Mach numbers.

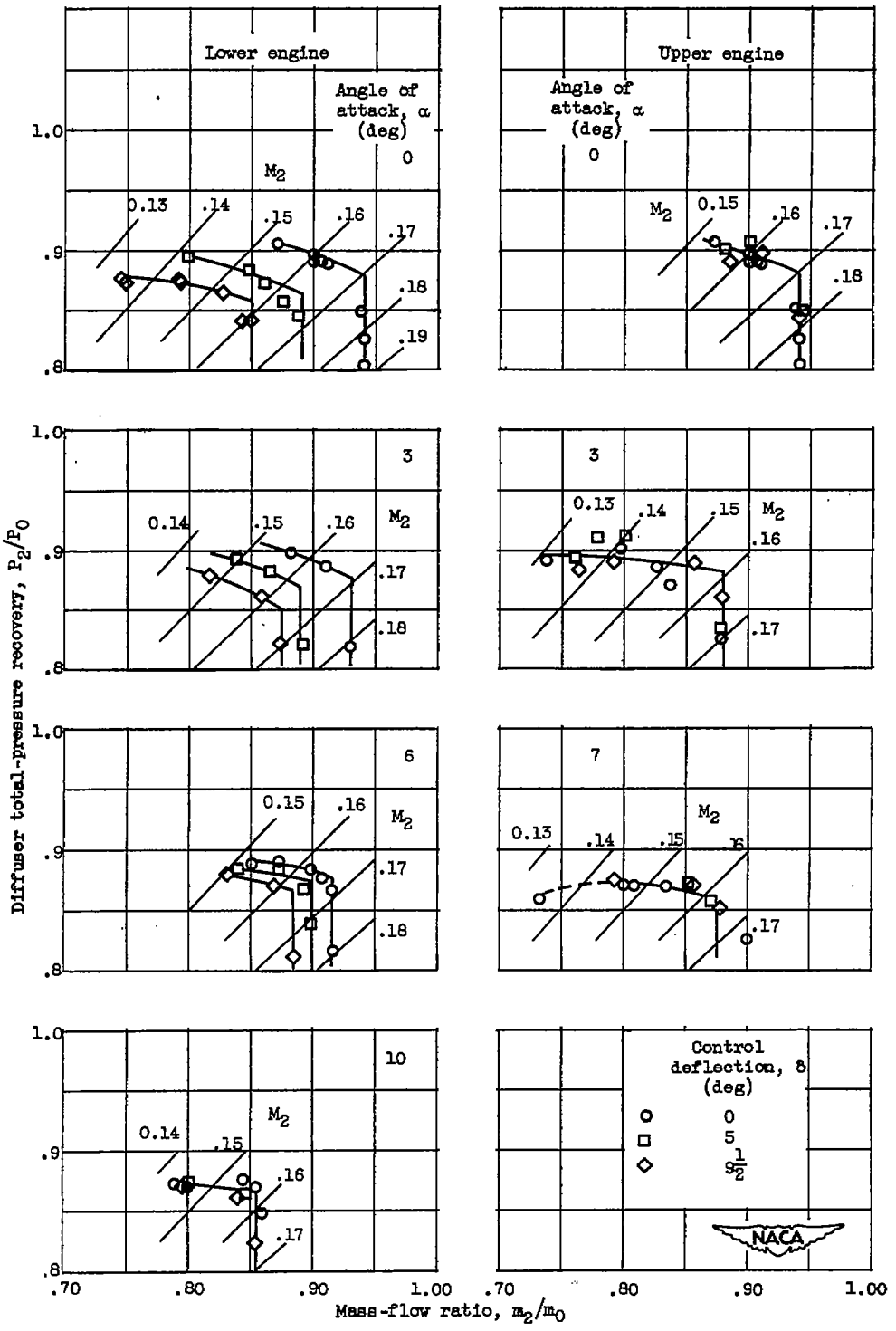

(b) M_0 = 1.8.

Figure 11. - Continued. Variation of total-pressure recovery with mass-flow ratio for upper and lower engines at several angles of attack for three Mach numbers.

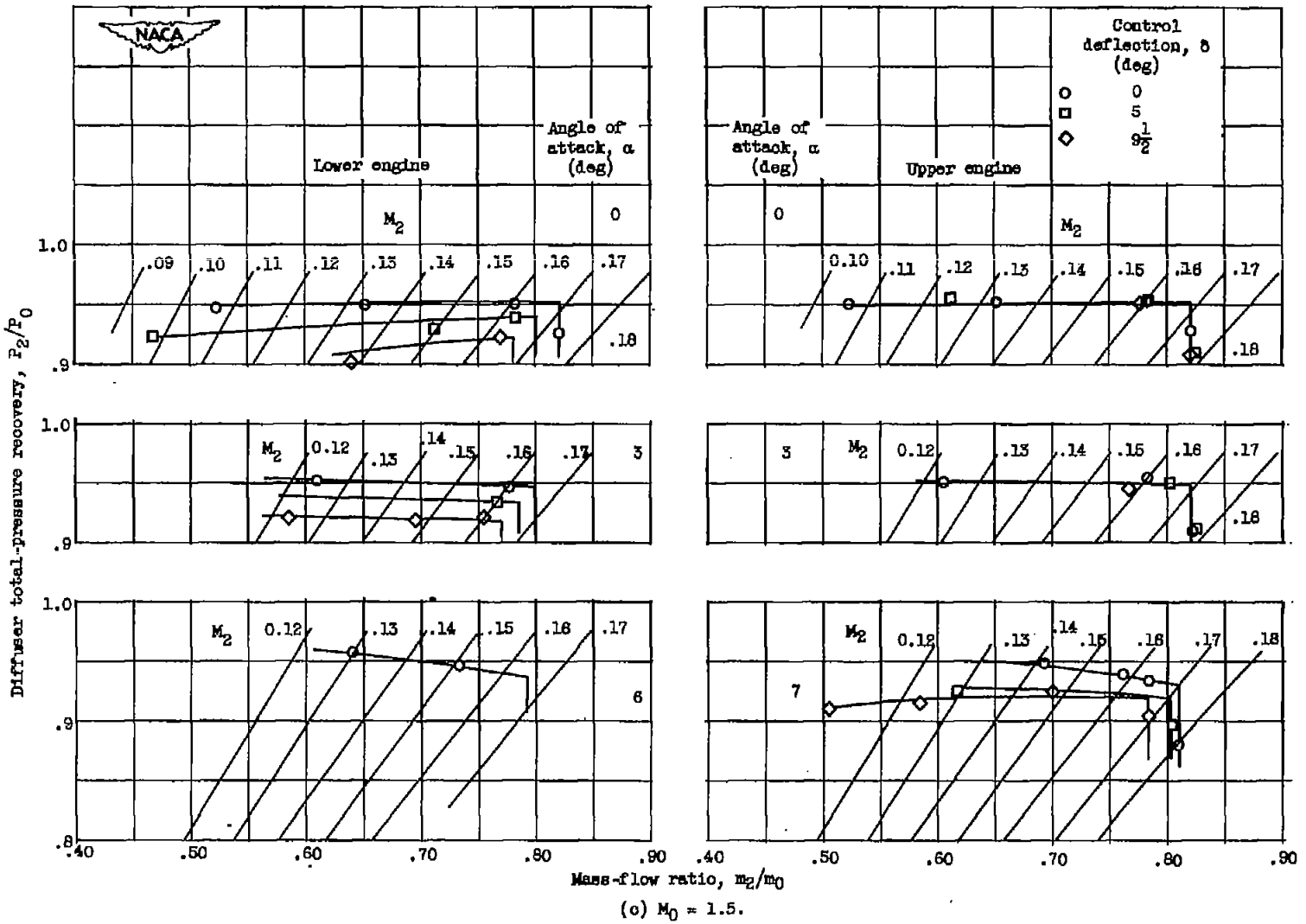

(c) $M_0 = 1.5$.

Figure 11. - Concluded. Variation of total-pressure recovery with mass-flow ratio for upper and lower engines at several angles of attack for three Mach numbers.